Coherent Interactions between Silicon-Vacancy Centers in Diamond

Matthew W. Day,[1] Kelsey M. Bates,[1] Christopher L. Smallwood,[1,2] Rachel C. Owen,[1] Tim Schröder,[3] Edward Bielejec,[4] Ronald Ulbricht,[5] and Steven T. Cundiff[1,*]

[1]*Department of Physics, University of Michigan, Ann Arbor, Michigan 48109, USA*
[2]*Department of Physics and Astronomy, San José State University, San Jose, California 95192, USA*
[3]*Department of Physics, Humboldt-Universität zu Berlin, Newtonstraße 15, 12489 Berlin, Germany*
[4]*Sandia National Laboratories, Albuquerque, New Mexico 87185, USA*
[5]*Max Planck Institut für Polymerforschung, Ackermannweg 10, 55128 Mainz, Germany*

(Received 22 April 2021; revised 11 March 2022; accepted 4 April 2022; published 17 May 2022)

We report tunable excitation-induced dipole-dipole interactions between silicon-vacancy color centers in diamond at cryogenic temperatures. These interactions couple centers into collective states, and excitation-induced shifts tag the excitation level of these collective states against the background of excited single centers. By characterizing the phase and amplitude of the spectrally resolved interaction-induced signal, we observe oscillations in the interaction strength and population state of the collective states as a function of excitation pulse area. Our results demonstrate that excitation-induced dipole-dipole interactions between color centers provide a route to manipulating collective intercenter states in the context of a congested, inhomogeneous ensemble.

DOI: 10.1103/PhysRevLett.128.203603

Entangled ensembles of quantum systems are a key resource for quantum sensing [1,2] and quantum information networks [3,4]. Color centers in diamond show potential as a physical realization of this resource. These point defects in the diamond lattice host localized and optically accessible atomlike electronic states, featuring favorable spin and optical coherence properties. Negatively charged silicon-vacancy centers in diamond (SiV^-), a class of color center, are largely protected by symmetry from the optical inhomogeneity that plagues the more heavily studied nitrogen-vacancy centers. Moreover, SiV^- centers exhibit a sharp zero-phonon line (ZPL) into which a majority of their photoluminescence (PL) is concentrated [5–10].

Realizing multicenter entangled ensembles is a challenge, typically requiring sophisticated device engineering to enhance weak photon-mediated interactions between isolated, implanted centers [4,11]. One alternative approach is to utilize entanglement generated ambiently between these emitters in dense ensembles through excitation-induced electronic dipole interactions [12–14]. Only sparse evidence in this direction exists in color center ensembles: evidence of superradiance has been reported in nitrogen vacancy centers [15] by observing a change in PL lifetime with increasing center density, but the difficulty of identifying the excitation level or degree of coherence in the ensemble makes attributing this change to interaction-generated multicenter collective states challenging. This challenge is surmountable, because excitation-induced shifts (EIS) and excitation-induced dephasing (EID) caused by interactions between emitters can tag signals from entangled states composed of N excited emitters, even under semiclassical excitation. The resulting nonlinear wave-mixing signal caused by interaction-induced shifts can be used to isolate the optical response of collective multicenter states (which we term subensembles) with excitation level N from the larger ensemble [16].

We directly probe transition-induced electronic dipole-dipole interactions [12] between pairs of emitters within a dense ensemble of SiV^- centers at cryogenic temperatures (15 K) using double-quantum two-dimensional (DQ2D) coherent spectroscopy. This technique is a background-free signature of interactions, in the sense that in the absence of excitation-dependent interactions there is no DQ2D signal [17]. DQ2D coherent spectroscopy yields the ensemble-averaged optical response of pairwise coherent subensembles subjected to coherent driving by a pulsed laser. With the addition of a preceding pump pulse, we implement control of the intercenter, excitation-induced interaction strength through the manipulation of the jointly-excited-state population of energetically degenerate centers by tuning the pump pulse area. Both the interaction strength and the jointly excited population state oscillate with increasing pump pulse area, while the same is not true for interacting centers excited on nondegenerate transitions. This demonstration both provides a route to accessing entangled ensembles of quantum emitters via interaction-induced Dicke physics and shows that nonlinear wave mixing can be used to sensitively extract the dynamics of entangled SiV^- subensembles from the complex optical response of the ensemble.

Figure 1 summarizes the color center system. Figure 1(a) depicts the SiV^- center with the vacancy-vacancy axis

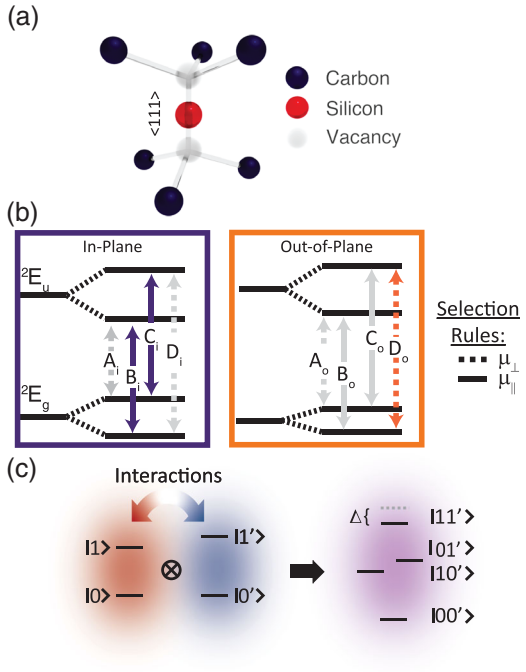

FIG. 1. (a) The SiV^- system: a silicon atom located between two vacancies. (b) The electronic level scheme with the ZPL transitions labeled. We do not consider hyperfine-split states, as these states are degenerate in the absence of a magnetic field, as is the case here. Polarization selection rules (dotted or dashed arrows) are depicted relative to the SiV^- axis; gray arrows show missing transitions. (c) A depiction of how excitation-dependent interactions couple two systems, modifying the properties of their jointly excited state captured by the complex-valued interaction parameter Δ.

orientation falling along the $\langle 111 \rangle$ direction in the lattice. The SiV^- zero-phonon line transitions probed with DQ2D are marked B_i, C_i, and D_o in Fig. 1(b). In this sample, due to its (110) orientation and due to strain and geometry considerations, the polarization selection rules yield PL from only these three transitions for X-polarized excitation (horizontal with respect to the experimental axes) [18]. Transitions B_i and C_i yield PL collected from centers oriented in the plane of the sample whereas transition D_o yields PL originating from centers oriented out of the plane of the sample, as the averaged bulk strain shifts the peak locations for different center orientations relative to each other [18].

To extract spectroscopic information about the interacting center pairs, DQ2D employs four pulses derived from a titanium sapphire oscillator (center wavelength 735 nm, repetition rate 75.5 MHz, pulse width 200 fs full-width, half maximum). Pulses are individually phase cycled with acousto-optic modulators to allow for the selection of multiple linear or nonlinear signal pathways. The four pulses illuminate the sample colinearly, generating nonlinear polarizations and modulated populations in the SiV^- electronic states [19–22]. The sample is an ensemble implanted in a (110)-oriented diamond crystal with SiV^- implantation density $\sim 10^{18}$ cm^{-3} tilted at a 30° angle to the horizontal. The modulated population due to the action of four pulses results in a modulated PL signal, collected in reflection [22]. Further sample-specific and experiment-specific details can be found in Refs. [18,23] and in the Supplemental Material of Ref. [22]. The four-wave mixing (FWM) pathway is selected by phase-synchronous detection of the fourth-order PL modulation at $\omega_{sig} = \omega_1 + \omega_2 - \omega_3 - \omega_4$.

Figure 2(a) is a schematic of a DQ2D signal pathway generated by this pulse sequence in a four-level "diamond"

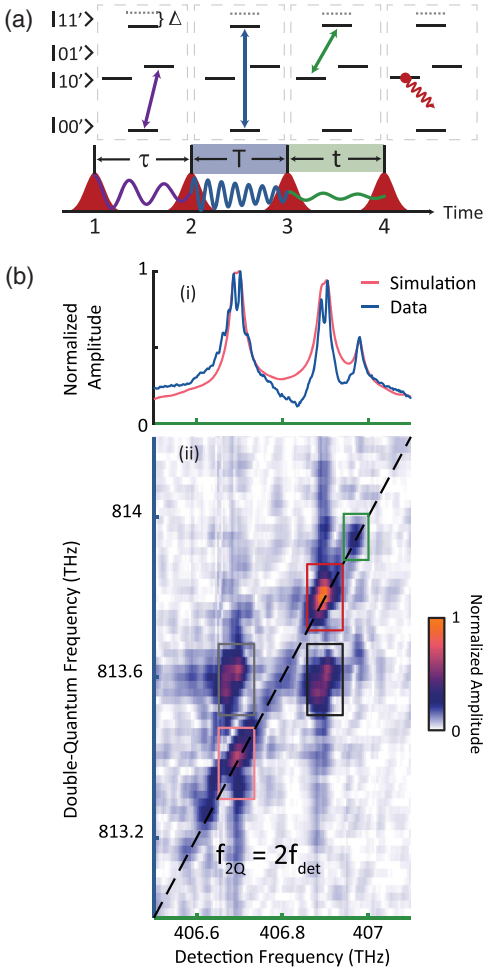

FIG. 2. (a) A diagram of the pulse sequence used in the DQ2D experiment. Arrows denote coherences established between states. Coherences between center pairs evolve during waiting time T, and their excitation-induced influence on the PL spectrum is resolved along waiting time t. (b)(i) A comparison between a linear PL spectrum and a simulation incorporating electronic dipole-dipole interactions as the broadening mechanism. (ii) A DQ2D spectrum from the SiV^- ensemble. Peaks in the pink, red, and green boxes arise from coherent coupling between two resonantly excited states. Nonresonant coherent coupling between centers yields peaks on either side of the diagonal, in the black and gray boxes.

energy level structure representing two interacting emitters. In this case, the first pulse drives a coherence between the ground and first excited state, which is converted by the second pulse into a "double-quantum" coherence between the ground and doubly excited state at twice the energy. For this reason, the frequency during time delay T is termed the "double-quantum" evolution of the FWM signal. The third and fourth pulses convert that coherence into a population in a singly (or doubly) excited state. The phase and amplitude of the PL modulation at ω_{sig} are monitored as a function of T and t, then Fourier transformed yielding two-dimensional spectra. The time delays corresponding to the Fourier transform of the two time axes are color coded in Fig. 2(a) and in Figs. 2(b)(i) and 2(b)(ii) .

A linear PL-detected absorption spectrum of the ZPL transitions is shown in Fig. 2(b)(i). Figure 2(b)(ii) is a DQ2D spectrum showing excitation-induced interactions between centers where the transitions are both degenerate and nondegenerate, as evidenced by peaks along the diagonal and off-diagonal directions, respectively. For completeness, a DQ2D spectrum taken for the orthogonal excitation polarization is included in the Supplemental Material [23]. As mentioned above, these peaks are a background-free signature of excitation-dependent interactions between centers.

The most likely mechanisms by which SiV^- centers interact are wave function overlap (Dexter coupling), electronic transition-induced dipole-dipole mediated interactions, spin-spin interactions, or phonon-mediated interactions. In the first case, one might expect an additional contribution to the DQ2D spectrum from the hybridized states [25]. We rule out this possibility, because the resulting spatially weak hybridization has not been seen to contribute to DQ2D spectra [26], and *ab initio* simulations of the electron wave functions in SiV^- centers do not show much spatial extent outside of roughly one unit cell, an order of magnitude less than required for significant spatial overlap between wave functions of adjacent centers at our implantation densities [9,27]. Although the SiV^- center electronic transition dipole moment of $\mu = 14.3$ Debye [6] is less than that in Rydberg atoms, the emitter densities achieved here are orders of magnitude larger than those of dilute gasses; thus, the comparatively weak transition dipole moment is compensated with higher emitter densities [6,28]. Furthermore, one might also consider spin-spin interactions in this system. However, these interactions are not strong enough to explain our findings: for two centers spaced roughly 10 nm apart, the spin-spin interaction shift is on the order of 10–100 kHz (depending on spin orientation), which is far too small to explain the observed inhomogeneity in the linear spectra and the excitation-induced shifts in the DQ2D spectra, which are both on the order of 10 GHz. To rule out phonon-mediated interactions between centers, we note that the electron-phonon dephasing times are expected to be on the order of 1–10 ps in ensembles SiV^- centers [10], and we observe double-quantum coherence times at least 5 times longer (on the order of 50 ps as estimated from a fit of the upper on-diagonal peak). We therefore conclude that the most likely interaction mechanism is electronic dipole-dipole coupling between adjacent centers.

Even in the complex SiV^- center energy level system, signal pathways in DQ2D spectra will be dominated by separate two-level systems interacting. A detailed argument for this assertion can be found in the Supplemental Material [23]. The conclusion is that the DQ2D line shape for a given pair of interacting states, following the conventions in Ref. [19], the state labeling scheme in Fig. 1(c), and assuming approximately delta-function pulses, is

$$S^{(3)}(\tau,\omega_T,\omega_t) = \frac{\mu_{10}^2\mu_{1'0'}^2}{8\hbar^3}\frac{e^{-i\Omega_{10'}\tau}+e^{-i\Omega_{01'}\tau}}{\omega_T-\Omega_{11'}-\Delta} \times\left(\frac{1}{\omega_t-\Omega_{01'}}-\frac{1}{\omega_t-\Omega_{01'}-\Delta} +\frac{1}{\omega_t-\Omega_{10'}}-\frac{1}{\omega_t-\Omega_{10'}-\Delta}\right) \quad (1)$$

where $\Omega_{ij}=\omega_{ij}-i\gamma_{ij}$ is the complex frequency associated with the transition from the ijth state to the ground state including phenomenological dephasing γ_{ij}, $\omega_{ij}=(E_{ij}-E_{0,0'})/\hbar$ is the transition center frequency, μ_{ij} is the dipole moment corresponding to the transition between the i and j states (assumed to be equal between centers), and $\Delta=\Delta_d-i\Delta_s$ is the complex interaction parameter. From Eq. (1), it is clear that the nonlinear signal exactly cancels when $\Delta=0$, in the case of noninteracting two-level systems, consistent with DQ2D coherent spectroscopy being a background-free probe of interactions.

Beyond just being a useful probe of interactions, the DQ2D line shape is highly sensitive to the interplay between inhomogeneous broadening and the average interaction strength between centers. This sensitivity can be seen by the dependence of the nonlinear DQ2D signal on ω_{ij}, γ_{ij}, and $\Delta=\Delta_s-i\Delta_d$. In the case that interactions between states reduce dephasing (known as excitation-induced narrowing), γ_{ij} (or $1/T_2^*$) and Δ_d have opposite signs, introducing a phase ambiguity in the signal.

We remove this line shape ambiguity by simply considering the linear PL-detected absorption spectrum, demonstrating that interactions could be the source of inhomogeneity in the PL spectrum. We know from previous studies on this sample that the PL linewidths are dominated by inhomogeneous broadening [22], so we monitor the PL modulated at a frequency $\omega_{\mathrm{sig}}=\omega_3-\omega_4$ while varying time delay t between the third and fourth pulses in our experiment. This yields a coherent linear spectrum corresponding to a PL-detected absorption measurement, presented in Fig. 2(b)(i). Details of the simulation of the linear PL spectrum can be found in the Supplemental

Material [23]. The simulation demonstrates that excitation-induced electronic dipole-dipole interactions between centers might be responsible for the inhomogeneity of the PL linewidths in our sample.

Transition-induced electronic dipole-dipole interactions can be expected to couple pairs of indistinguishable centers into entangled Dicke states [13,29]. Using a variable-strength pulse preceding our DQ2D pulses (pulses 1–4 in Fig. 2) by 1 ns, we observe oscillations in the peak amplitude and phase of the on-diagonal DQ2D peaks with varying pump field. However, the signal due to non-degenerate centers decays with increasing pump field. Figure 3(a) shows the integral of the peaks in the DQ2D spectra as denoted in the boxes in Fig. 2(b)(ii). When compared with single quantum coherent spectra, reported in the Supplemental Material [23], only the resonant interacting centers undergo such coherent Rabi oscillations. The total FWM signal is not dominated by the excitation-induced contribution; rather, the DQ2D contribution to the total FWM response demonstrates that centers whose interactions generate mutual coherence behave as collective

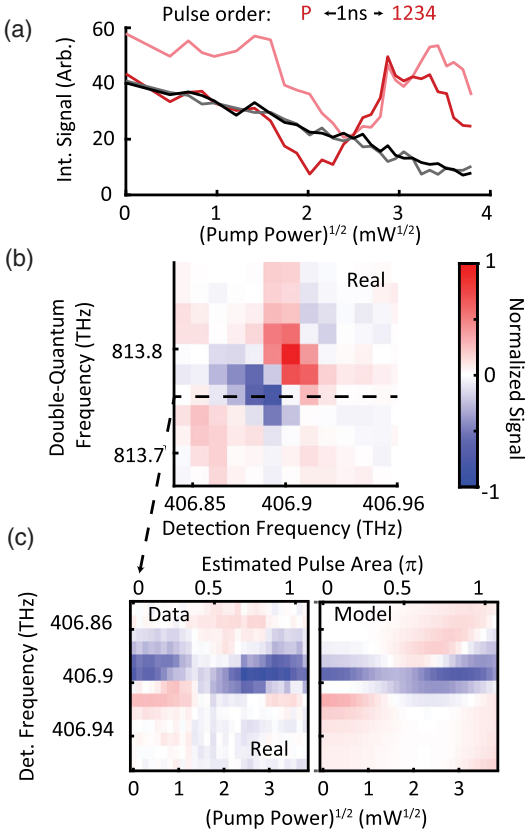

FIG. 3. (a) The integral of the unnormalized DQ2D peaks, integrated over the color-coded boxes in Fig. 2(b)(ii) as a function of pump field. (b) The phase-resolved zero-pump upper on-diagonal peak in the red box in Fig. 2(b)(ii). (c) Slices through the peak in (b) as a function of pump field as compared with a fit with our model, normalized such that zero is centered in the color scale to visually clarify the sign of the real component of the signal.

systems, and that excitation-induced interactions generate a DQ2D signal serving to "tag" coherent subensembles of color centers.

To explain this behavior, we posit that, as we tune the power of the pump pulse, we tune the population of center pairs (between the $|00'\rangle$ and the $|11'\rangle$ states) and thus also modify the excitation-induced interaction strength of the collective center pairs responsible for the DQ2D signal. The DQ2D signal oscillations likely arise only from excited center pairs. Dipole enhancement due to cooperation of three or more of color centers would act to smear out the coherent Rabi oscillations in the DQ2D signal. Given that the pump arrives 1 ns prior to the DQ2D coherent spectroscopy probe, the transition-induced interactions must persist at least this long to explain the behavior of the DQ2D spectra with increasing pump strength [23], indicating that the limiting factor impacting the usefulness of these collective states is their collective dephasing rate, which in this case is (at worst) twice that of the single-center rate observed in our sample. However, given the fact that dephasing times into the ns regime have been observed in these centers [24], and that correlations in dephasing mechanisms between emitters can dramatically lengthen the coherence time of their jointly excited states (likely for systems with closely spaced emitters such as SiV^- color centers [30]), these results carry general implications outside of the ultrafast regime.

We reproduce the qualitative behavior of the spectra by extracting and modelling a one-dimensional slice through the phase-resolved on-diagonal DQ2D peak. This captures both the change in interaction strength and population state incurred by center pairs due to their joint interaction with the incident pump pulse. We fit slices through the phase-resolved peak in the red box in Fig. 2(b)(ii), as shown in Figs. 3(b) and 3(c) as a function of power. The details of the model are summarized in the Supplemental Material [23]; the most salient detail is that the ground- and doubly excited-state populations of a four-level diamond system, representing two interacting color centers, scale with the driving field of a pump pulse as

$$\rho_{00'} \sim \cos\left(\frac{A}{2}\right)^4, \quad \rho_{11'} \sim \sin\left(\frac{A}{2}\right)^4 \tag{2}$$

where $A = \int_{-T_{\mathrm{rep}}/2}^{-T_{\mathrm{rep}}/2} d\tau \Omega(\tau)$ is the pulse area [31], $\Omega(\tau) = \vec{\mu} \cdot \vec{E}(\tau)/\hbar$ is the Rabi frequency with $\vec{\mu}$ the transition dipole moment, and $\vec{E}(\tau)$ the field of the pump pulse. The assumptions of the qualitative model are that the DQ2D signal is proportional to the ground-state population of the pairwise subensemble with interactions scaled linearly in accordance to the *jointly excited state* population for a given pump field, corresponding to the DQ2D signal pathways elaborated in Ref. [23]. Explicitly, this corresponds to assuming $S^{(3)}(\tau, \omega_T, \omega_t) \sim \cos^4(E/E_\pi)$ and $\Delta = \Delta_{s,0} - i\Delta_{d,0} + \sin^4(E/E_\pi)(\Delta_{s,1} - i\Delta_{d,1})$ where we assume

some residual EIS and EID during the DQ2D experiment as quantified in the parameters $\Delta_{s,0}$ and $\Delta_{d,0}$ to account for the zero-pump DQ2D signal. We label $\Delta_{s,1}$ and $\Delta_{d,1}$ to be the slope of the induced interaction shifts and changes in dephasing respectively. E_π is a scaling fit parameter such that when the pulse area is that of a "π" pulse, $E/E_\pi = \pi/2$.

The fit, shown in Fig. 3(c), captures the Rabi oscillations in peak strength and phase due to changes in both the population state and interaction strength of joint center pairs. After geometric, Fresnel, and optical spot size corrections (see the Supplemental Material [23]) we estimate the average pump power required for a pulse area of π in our model is $P_\pi = 9.6$ mW, in agreement with the theoretical value of $P_{\pi,\mathrm{thy}} = 9.86$ mW considering a repetition rate of 75.5 MHz and an estimated full-width half maximum pulse duration of 200 fs. The fit returns $\Delta_{d,0} = 2$ GHz, $\Delta_{s,0} = 6$ GHz, $\Delta_{d,1} = 50$ GHz, and $\Delta_{s,1} = -200$ GHz, in agreement with an estimation of $\Delta_{s,0} \approx \mathrm{O}(1-10)$ GHz retrieved from the simulations of the linear spectra [23].

The data presented here reveal that distinct SiV^- centers in ensembles interact through excitation-induced electronic dipole-dipole interactions. These tunable interactions persist for at least 1 ns and subsequently modify the central frequency and dephasing properties of the color center optical resonances, tagging the Dicke level of pairwise subensembles. Upon excitation with a pump pulse, these interaction-entangled center pairs undergo coherent oscillations in both their mutual interaction strength and population state. Similar phenomena have been seen in Rydberg atoms [28], but the present work constitutes an important demonstration of coherent control of collective states of multiple color centers in an adaptable solid-state platform.

This demonstration of Dicke physics is complementary to other works demonstrating coherent manipulation of color center nuclear spins using spin-spin (i.e., magnetic) interactions between a particular spin and nearby optically addressable electronic spins [32–34] achieved with high densities of nitrogen-vacancy centers. Before the practical utilization of these tunable interactions can become a reality, however, more must be understood about the dephasing mechanisms, population dynamics, and manipulation fidelity of entangled, proximate SiV^- centers. Extending this work by employing photon-counting nonlinear spectroscopy [35] to study DQ2D spectra as a function of pump delay, center density, and pump power would provide much insight into these questions.

The data that support the findings of this study are available from the corresponding author upon reasonable request.

We thank A. Liu and E. W. Martin for helpful discussions. T. S. acknowledges support from the Federal Ministry of Education and Research of Germany (BMBF, Project No. DiNOQuant, 13N14921). Ion implantation work to generate the SiV centers was performed, in part, at the Center for Integrated Nanotechnologies, an Office of Science User Facility operated for the U.S. Department of Energy (DOE) Office of Science. Sandia National Laboratories is a multimission laboratory managed and operated by National Technology and Engineering Solutions of Sandia, LLC., a wholly owned subsidiary of Honeywell International, Inc., for the U.S. Department of Energy's National Nuclear Security Administration under Contract No. DE-NA-0003525. This paper describes objective technical results and analysis. Any subjective views or opinions that might be expressed in the paper do not necessarily represent the views of the U.S. Department of Energy or the United States Government. C. L. S. acknowledges support from the National Science Foundation under Grant No. 2003493.

*cundiff@umich.edu

[1] C. L. Degen, F. Reinhard, and P. Cappellaro, Quantum sensing, Rev. Mod. Phys. **89**, 035002 (2017).
[2] J. F. Barry, J. M. Schloss, E. Bauch, M. J. Turner, C. A. Hart, L. M. Pham, and R. L. Walsworth, Sensitivity optimization for NV-diamond magnetometry, Rev. Mod. Phys. **92**, 015004 (2020).
[3] H. J. Kimble, The quantum internet, Nature (London) **453**, 1023 (2008).
[4] A. Sipahigil, R. E. Evans, D. D. Sukachev, M. J. Burek, J. Borregaard, M. K. Bhaskar, C. T. Nguyen, J. L. Pacheco, H. A. Atikian, C. Meuwly, R. M. Camacho, F. Jelezko, E. Bielejec, H. Park, M. Lončar, and M. D. Lukin, An integrated diamond nanophotonics platform for quantum-optical networks, Science **354**, 847 (2016).
[5] A. Dietrich, K. D. Jahnke, J. M. Binder, T. Teraji, J. Isoya, L. J. Rogers, and F. Jelezko, Isotopically varying spectral features of silicon-vacancy in diamond, New J. Phys. **16** (2014).
[6] J. N. Becker and C. Becher, Coherence properties and quantum control of silicon vacancy color centers in diamond, Phys. Status Solidi A **214**, 1 (2017).
[7] E. Londero, G. Thiering, L. Razinkovas, A. Gali, and A. Alkauskas, Vibrational modes of negatively charged silicon-vacancy centers in diamond from *ab initio* calculations, Phys. Rev. B **98**, 035306 (2018).
[8] S. Meesala, Y.-I. Sohn, B. Pingault, L. Shao, H. A. Atikian, J. Holzgrafe, M. Gündogan, C. Stavrakas, A. Sipahigil, C. Chia, R. Evans, M. J. Burek, M. Zhang, L. Wu, J. L. Pacheco, J. Abraham, E. Bielejec, M. D. Lukin, M. Atatüre, and M. Loncar, Strain engineering of the silicon-vacancy center in diamond, Phys. Rev. B **97**, 205444 (2018).
[9] P. Udvarhelyi, R. Nagy, F. Kaiser, S.-Y. Lee, J. Wrachtrup, and A. Gali, Spectrally Stable Defect Qubits with No Inversion Symmetry for Robust Spin-to-Photon Interface, Phys. Rev. Applied **11**, 044022 (2019).
[10] A. Liu and S. T. Cundiff, Spectroscopic signatures of electron-phonon coupling in silicon-vacancy centers in diamond, Phys. Rev. Mater. **4**, 055202 (2020).

[11] N. H. Wan, T. J. Lu, K. C. Chen, M. P. Walsh, M. E. Trusheim, L. De Santis, E. A. Bersin, I. B. Harris, S. L. Mouradian, I. R. Christen, E. S. Bielejec, and D. Englund, Large-scale integration of artificial atoms in hybrid photonic circuits, Nature (London) **583**, 226 (2020).
[12] G. W. King and J. H. van Vleck, Dipole-dipole resonance forces, Phys. Rev. **55**, 1165 (1939).
[13] G. K. Brennen, I. H. Deutsch, and P. S. Jessen, Entangling dipole-dipole interactions for quantum logic with neutral atoms, Phys. Rev. A **61**, 062309 (2000).
[14] E. R. Hudson and W. C. Campbell, Dipolar quantum logic for freely rotating trapped molecular ions, Phys. Rev. A **98**, 040302(R) (2018).
[15] C. Bradac, M. T. Johnsson, M. v. Breugel, B. Q. Baragiola, R. Martin, M. L. Juan, G. K. Brennen, and T. Volz, Room-temperature spontaneous superradiance from single diamond nanocrystals, Nat. Commun. **8**, 1205 (2017).
[16] D. Liang and H. Li, Optical two-dimensional coherent spectroscopy of many-body dipoledipole interactions and correlations in atomic vapors, J. Chem. Phys. **154**, 214301 (2021).
[17] J. Kim, S. Mukamel, and G. D. Scholes, Two-dimensional electronic double-quantum coherence spectroscopy., Acc. Chem. Res. **42**, 1375 (2009).
[18] K. M. Bates, M. W. Day, C. L. Smallwood, R. C. Owen, T. Schrder, E. Bielejec, R. Ulbricht, and S. T. Cundiff, Using silicon-vacancy centers in diamond to probe the full strain tensor, J. Appl. Phys. **130**, 024301 (2021).
[19] C. Smallwood, T. Autry, and S. Cundiff, Analytical solutions to the finite-pulse Bloch model for multi-dimensional coherent spectroscopy, J. Opt. Soc. Am. B **34** (2016).
[20] P. F. Tekavec, G. A. Lott, and A. H. Marcus, Fluorescence-detected two-dimensional electronic coherence spectroscopy by acousto-optic phase modulation, J. Chem. Phys. **127**, 214307 (2007).
[21] G. Nardin, T. M. Autry, K. L. Silverman, and S. T. Cundiff, Multidimensional coherent photocurrent spectroscopy of a semiconductor nanostructure., Opt. Express **21**, 28617 (2013).
[22] C. L. Smallwood, R. Ulbricht, M. W. Day, T. Schröder, K. M. Bates, T. M. Autry, G. Diederich, E. Bielejec, M. E. Siemens, and S. T. Cundiff, Hidden Silicon-Vacancy Centers in Diamond, Phys. Rev. Lett. **126**, 213601 (2021).
[23] See Supplemental Material at http://link.aps.org/supplemental/10.1103/PhysRevLett.128.203603 and references therein.
[24] L. J. Rogers, K. D. Jahnke, M. W. Doherty, A. Dietrich, L. P. McGuinness, C. Müller, T. Teraji, H. Sumiya, J. Isoya, N. B. Manson, and F. Jelezko, Electronic structure of the negatively charged silicon-vacancy center in diamond, Phys. Rev. B **89**, 235101 (2014).
[25] J. F. Specht, A. Knorr, and M. Richter, Two-dimensional spectroscopy: An approach to distinguish Förster and Dexter transfer processes in coupled nanostructures, Phys. Rev. B **91**, 155313 (2015).
[26] G. Nardin, G. Moody, R. Singh, T. M. Autry, H. Li, F. Morier-Genoud, and S. T. Cundiff, Coherent Excitonic Coupling in an Asymmetric Double InGaAs Quantum Well Arises from Many-Body Effects, Phys. Rev. Lett. **112**, 046402 (2014).
[27] A. Gali and J. R. Maze, *Ab initio* study of the split silicon-vacancy defect in diamond: Electronic structure and related properties, Phys. Rev. B **88**, 235205 (2013).
[28] Y. O. Dudin, L. Li, F. Bariani, and A. Kuzmich, Observation of coherent many-body Rabi oscillations, Nat. Phys. **8**, 790 (2012).
[29] R. H. Dicke, Coherence in spontaneous radiation processes, Phys. Rev. **93**, 99 (1954).
[30] B. Lomsadze and S. T. Cundiff, Line-shape analysis of double-quantum multidimensional coherent spectra, Phys. Rev. A **102**, 043514 (2020).
[31] S. L. McCall and E. L. Hahn, Self-induced transparency, Phys. Rev. **183**, 457 (1969).
[32] J. Choi, S. Choi, G. Kucsko, P. C. Maurer, B. J. Shields, H. Sumiya, S. Onoda, J. Isoya, E. Demler, F. Jelezko, N. Y. Yao, and M. D. Lukin, Depolarization Dynamics in a Strongly Interacting Solid-State Spin Ensemble, Phys. Rev. Lett. **118**, 093601 (2017).
[33] S. Choi, J. Choi, R. Landig, G. Kucsko, H. Zhou, J. Isoya, F. Jelezko, S. Onoda, H. Sumiya, V. Khemani, C. von Keyserlingk, N. Y. Yao, E. Demler, and M. D. Lukin, Observation of discrete time-crystalline order in a disordered dipolar many-body system, Nature (London) **543**, 221 (2017).
[34] G. Kucsko, S. Choi, J. Choi, P. C. Maurer, H. Zhou, R. Landig, H. Sumiya, S. Onoda, J. Isoya, F. Jelezko, E. Demler, N. Y. Yao, and M. D. Lukin, Critical Thermalization of a Disordered Dipolar Spin System in Diamond, Phys. Rev. Lett. **121**, 023601 (2018).
[35] K. E. Dorfman and S. Mukamel, Time-and-frequency-gated photon coincidence counting: A novel multidimensional spectroscopy tool, Phys. Scr. **91**, 083004 (2016).